FUGRO GEOSAR AIRBORNE DUAL-BAND IFSAR DTM PROCESSING

Bert Kampes, Megan Blaskovich, James. J. Reis, Mark Sanford, Kevin Morgan
Fugro EarthData, Inc.
Frederick, MD 21704, USA
bkampes@earthdata.com

ABSTRACT

This paper presents Fugro EarthData's GeoSAR airborne, single-pass, dual-band Interferometric Synthetic Aperture Radar (IFSAR) system's technical details and preliminary processing results in relation to the Alaska Statewide Digital Mapping Initiative (SDMI). The focus of this paper is on how data were acquired, processed and validated to produce the three key products at 5 m posting: the Digital Terrain Model (DTM), the Digital Surface Model (DSM), and the X-band Orthorectified Radar Magnitude Imagery (ORI or MAG). GeoSAR incorporates a nadir-looking profiling LiDAR, from which 48,433 points in the Pilot Area are analyzed. Using these LiDAR measurements, the RMSEz of the DTM is estimated to be 1.11 m for terrain slopes between 0°–10°, and 1.54 m overall, including 2,035 points on slopes >30°.

KEYWORDS: Fugro GeoSAR airborne Dual-Band IFSAR, LiDAR, Alaska, DTM, DSM, DEM

INTRODUCTION

The GeoSAR system acquired data in late July 2010 in the Project Area in Alaska, shown in Fig. 1, as part of the Alaska Statewide Digital Mapping Initiative, SDMI (Maune, 2008; 2009; 2010). The project is only briefly introduced here, because detailed information is available in the 2011 ASPRS special session on Large Scale Mapping: Alaska Statewide Mapping Refresh – Overview and Current Status.

It is stated in the *Alaska Whitepaper* (Maune, 2008, page 2) that: "The current NED* for Alaska is both lower resolution and lower accuracy (both vertically and horizontally) than that for the contiguous lower-48 states. In addition to vertical inaccuracies of hundreds of meters, entire mountain ranges are known to be horizontally misplaced by as much as two nautical miles, making it extremely difficult to use the NED for the simplest task – orthorectification of imagery. […] The current NED for Alaska does not satisfy Alaska user requirements and national priorities as identified during the user surveys […]".

Under this USGS contract, the deliverable products for the Alaska Digital Elevation Models are the DTM, DSM and Orthorectified Magnitude Imagery, summarized in Table 1. The main product is the DTM with 20-foot equivalent contour accuracy, corresponding to RMSEz=1.85 m and RMSEr=8.03 m (5.6 m in Northing and Easting) for the vertical and horizontal accuracy, respectively. The data are delivered in Alaska Albers projection with 5 m post spacing, and in HRTe3 format in geographic projection. The DEMs values are orthometric height, using the NGS Geoid09 model, and hydrologically enforced (rivers monotonically flowing down and lakes flattened, size >50×150m^2). These products will become public domain, when published by the USGS in the NED.

Airborne IFSAR was selected as the most appropriate technology that cost-efficiently can provide high quality data products, fulfilling the requirements of the federal and Alaska stake holders. A number of typical GeoSAR products are not part of the deliverables, in particular:

- P-band magnitude imagery for HH and HV polarization, as well as full-pol and derived products.
- P-band interferometrically derived heights (the DTM heights are based on P-band and X-band data, i.e., on bare earth for example it is a combination, while in vegetated areas it is mainly P-band based, but, for example, glacier DTM elevations are based on X-band, as the P-band data penetrates the glacier surface [Morgan, 2011].)
- Higher-resolution or colorized orthorectified magnitude imagery.

* National Elevation Dataset, produced and distributed by the U.S. Geological Survey (USGS).

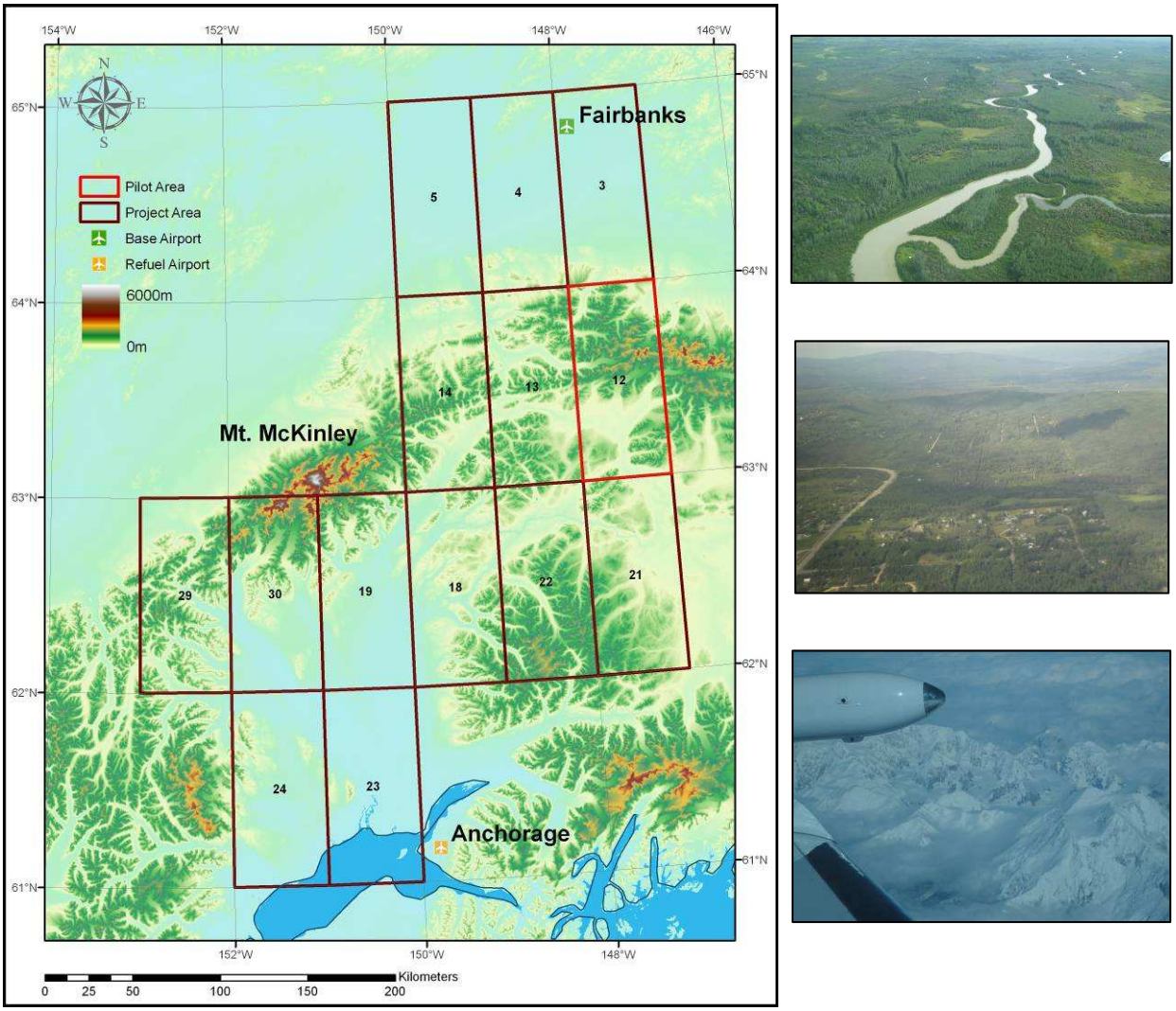

Figure 1. Project Area, covering Fairbanks, Anchorage, and Mt. McKinley (Denali). The numbers refer to the priority of 1 degree cells given by the USGS. The panel on the right shows examples of highly varying terrain types and mixed land cover in the Project Area, from flat and forested, to hilly, to mountainous and snow and ice covered.

Table 1. Main Project Deliverables. Data are posted at 5 m, Alaska Albers projection.

Product	Description	GeoSAR Observations
DTM	▪ Digital Terrain Model ▪ Geoid09 Orthometric Heights ▪ Vegetation and Buildings Removed ▪ Hydrologically Enforced	▪ P-band and X-band Interferometry ▪ Multiple Looks
DSM	▪ Digital Surface Model ▪ Geoid09 Orthometric Heights ▪ Hydrologically Enforced	▪ Based on X-Band Interferometry ▪ Multiple Looks
ORI	▪ Orthorectified Radar Magnitude Image ▪ Multiple view directions average	▪ X-band ▪ Multiple Looks
Masks	▪ Quality Masks ▪ Hydrology, Voids, Fills, Slope category	▪ P-band and X-band
Meta	▪ Meta Information	▪ FDGC compliant

GEOSAR SYSTEM

GeoSAR is a unique, state-of-the-art, dual-band, dual-sided, single-pass interferometric mapping radar designed to efficiently map, wide-area, both top vegetation canopies and the terrain beneath the canopy. The GeoSAR system was developed from 1998-2003 as a joint effort of NASA JPL and Fugro EarthData under sponsorship of DARPA and NGA (Wheeler and Hensley, 2000; Reis et al., 2009). The X-band radar has VV polarization and a carrier center frequency of 9.7 GHz, and the P-band radar is centered at 0.35 GHz, both with a 160 MHz bandwidth. The P-band is fully polarimetric-interferometric, and HH and HV data are recorded in the topographic mapping mode as used for this project.

The GeoSAR system is flown on a Gulfstream II jet aircraft and maps swaths simultaneously on both sides of the aircraft to generate high quality DEMs and imagery at both X-band and P-band. The nominal field of view is between 25° and 60°, corresponding to 10–15 km swath width, depending on flying altitude above the terrain, see also Fig. 2. The system was augmented in 2005 with a modified Leica ALS-40 nadir-pointing LiDAR profiler system to measure highly accurate ground control points that are used during production of large area mosaics and as validation control. The LiDAR is specified to have a vertical accuracy of better than 30 cm from altitudes up to 13,000 m (Hoffman, 2006), and was recently validated to have approximately 15 cm precision (one sigma), derived using a total of ~21,000 points at two independent ground data sites in Georgia and South Carolina, where high-accuracy ground data were available (EarthData, 2010). The GeoSAR LiDAR is used in this paper to validate the DEM products in the Alaska Pilot Area.

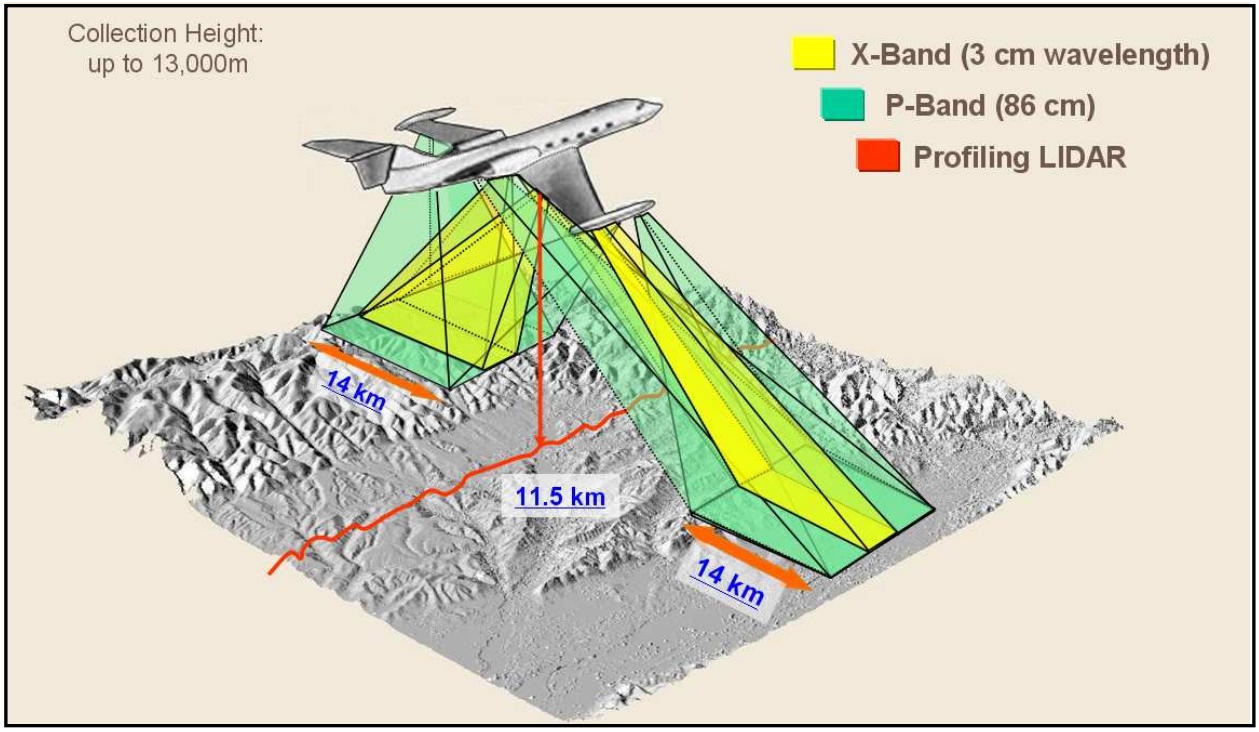

Figure 2. GeoSAR system overview. The GeoSAR radar flies aboard a Gulfstream-II modified jet at high altitude and high-speed. This configuration makes it efficient for wide-area mapping applications, acquiring data on both sides of the plane simultaneously in X-band and P-band at a rate of approximately 300 km^2 per minute, per band (~400 MB per second).

As is well known, see for example (Rosen et al., 2000; Kampes, 2006; Meyer et al., 2005), a single-pass radar can "see" through clouds and in the dark, and height estimation is not affected by atmospheric heterogeneities, as is a repeat-pass system. Being dual-sided, the GeoSAR system maps approximately 12–15 km wide swaths on both sides of the aircraft, from a nominal altitude of 39,500 feet (above Mean Sea Level), under a field of view of 25°–60°. The exact swath width depends on the altitude above terrain, as well as from the maximum look-angle used during processing (the GeoSAR system records approximately 25 km of slant-range returns, data is recorded from nadir to much farther than the nominal 60° used for standard product generation).

Table 2. Main GeoSAR characteristics.

Property	Advantage
▪ Fugro	▪ Expertise and stability of project management and quality processes. Full data ownership
▪ Gulfstream-II platform	▪ High-altitude, efficient wide area mapping suitable for flat terrain and extreme terrain
▪ Single-Pass	▪ No atmospheric errors or temporal decorrelation, operating in all-weather, day and night
▪ Dual-Band (X+P)	▪ Simultaneous mapping above and below the foliage for elevation and feature extraction (mapping)
▪ Dual-Baseline (SAT+PP)	▪ Reliability enhanced by additional height estimations and flexibility to use the proper processing mode for the product at hand
▪ Dual-Side (L+R)	▪ Efficient and reliable mapping to get fast coverage and reduced shadow and layover, particularly in rough terrain.
▪ Quad-Pol (HH, HV, VH, VV)	▪ Added value of interferometric polarimetry for a wide range of uses
▪ Profiling LiDAR	▪ Simultaneous reliable high-accurate ground control measurements provide on-board vertical control

Aside from the acquisition coverage advantage (twice more data per flight hour), the true advantage of a dual-sided system is the automatic acquisition of multiple measurements in mountainous terrain from different observation angles. Specifically, the problem of layover and shadow is significantly mitigated by a dual-sided system, because a pixel on the ground is observed under different angles. Moreover, the inherent redundancy provided by the dual-sided system increases the reliability, i.e., the ability to detect incorrect estimates, and reduces the errors of the estimated elevations. The dual-bands are the X-band and P-band. The X-band data are the basis for the DSM product, as the ~3 cm wavelength reflects off the first surface. The P-band data (~86 cm wavelength) are the basis for the DTM product as it significantly penetrates vegetation, making measurements of the elevations below the canopy.

Fig. 3 shows an alternate view of the number of looks of a given pixel on the ground, by considering the "opening angle" into the sky of the pixel on the ground, instead of the look angle looking down from the plane. For wide area mapping, parallel mapping lines with spacing of 4–7 km are normally used. The black arrows in Fig. 3 show the area in the sky in which the plane would observe the point on the ground. Typically there are 4 mapping lines in which the point is observed, i.e., the point is typically observed from four different directions, for example, two from the East and two from the West for North-South mapping lines. Fig. 3 also indicates that both X-band and P-band single-pass interferometric data are acquired, both in Single-Antenna-Transmit (SAT) mode and Ping-Pong mode (ULS, for example, is a mnemonic used to indicate UHF, P-band, Left side, SAT mode), see also (Reis, 2009). This means that there are typically 16 possible measurements of the interferometric height of a pixel, which greatly increases the ability to identify incorrect estimations and the ability to correct for them.

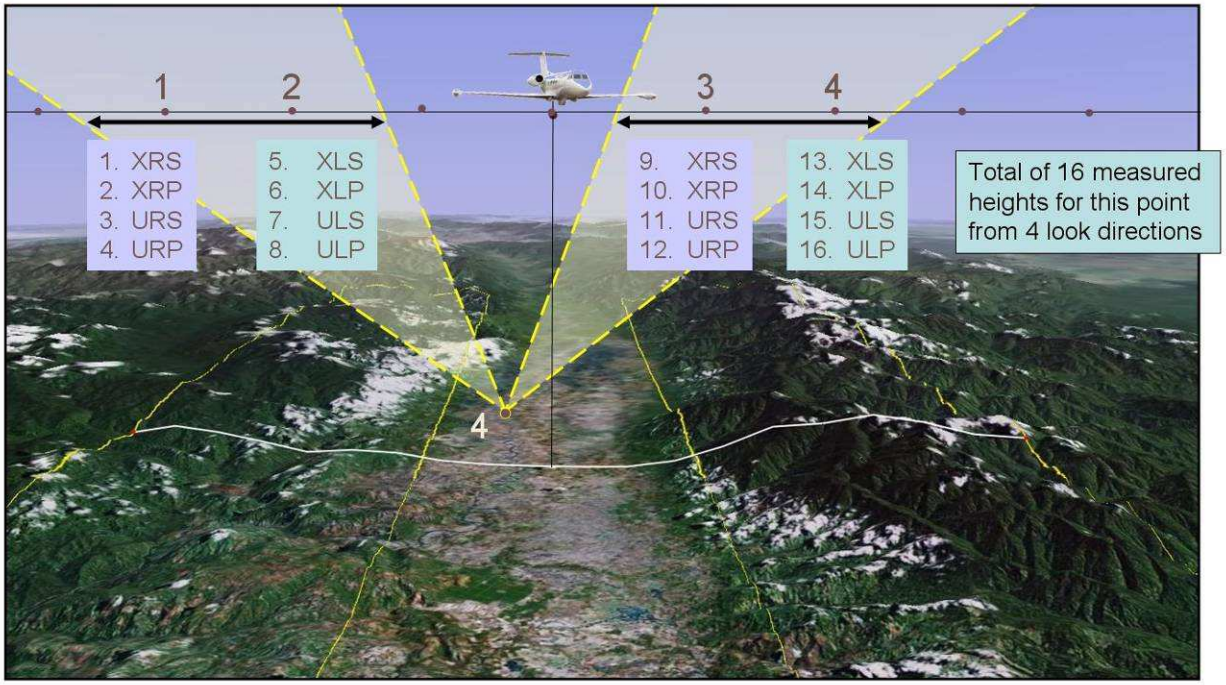

Figure 3. GeoSAR dual-band, dual-look, dual-baseline redundancy. A point on the ground is typically observed from four different directions (either from the Left or Right, depending on flight direction), each in four different interferometric modes (X-band and P-band, in Single-Antenna-Transmit and Ping-Pong mode), leading to 16 elevation estimations per pixel. The sketched nadir-looking profiling LiDAR provides independent ground control of the terrain directly below the flight path.

POSITIONAL ACCURACY ASSESSMENT USING LIDAR

The GeoSAR profiling LiDAR is a powerful tool to assess the horizontal and vertical accuracy of the delivered products. A total of 12,628,042 usable LiDAR points were available in the Pilot Area, see also Fig. 4. These points are remaining after eliminating all LiDAR points with an elevation higher than the maximum elevation in the Pilot Area, i.e., the data were cleaned from cloud returns. As the LiDAR data are acquired directly below the aircraft, the pattern of North-South mapping lines and orthogonal cross-ties is visible in Fig. 4. Locations that do not show LiDAR points were flown in cloudy conditions, as the GeoSAR radar is not affected by clouds, and data acquisition continues under such circumstances.

The LiDAR is designed to have a repeat precision of better than 30 cm vertical (one sigma), see also (Hoffmann, 2006). The LiDAR footprint is 3–5 m, depending on height above the terrain, and the sample density is approximately 3 cm, with 3-returns and 3 intensities. The horizontal accuracy (RMSE) of the LiDAR is about half the footprint.

To examine the repeatability of the LiDAR, a statistic is computed using cross-over points of independent data flights, as indicated in Fig. 4. The results of this test are shown in Table 3. In this simple manner the RMSEz of the repeat accuracy of the LiDAR is estimated as 39 cm.

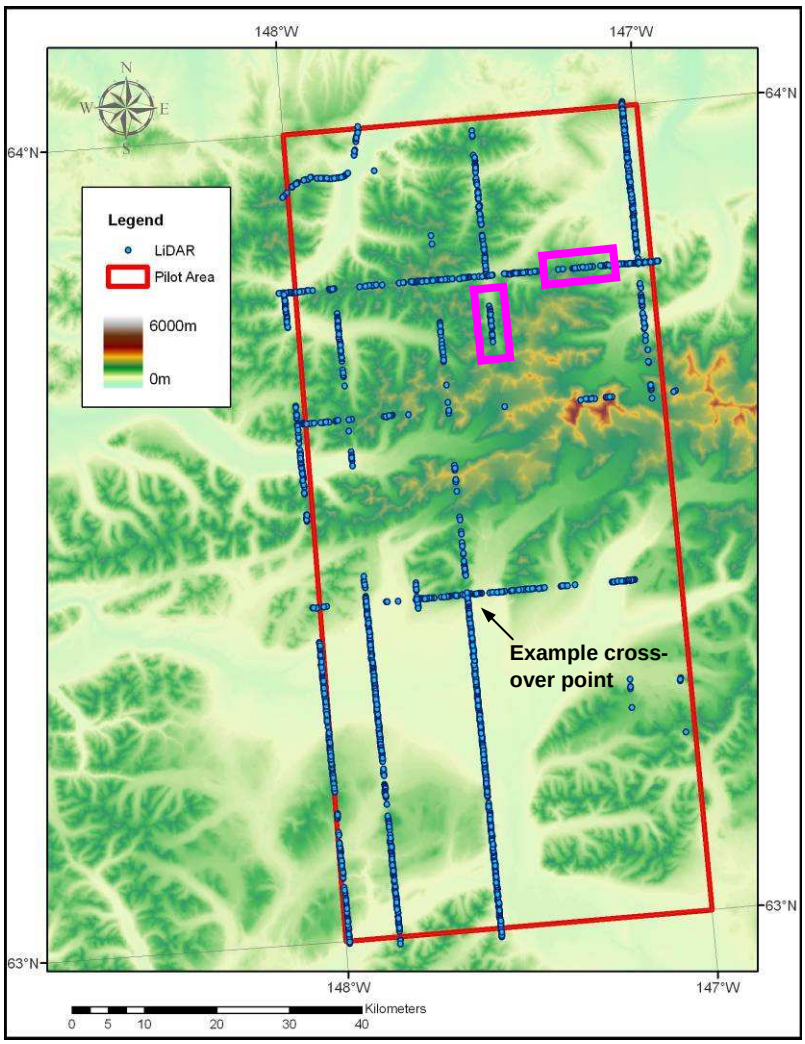

Figure 4. LiDAR points used for product quality assessment. Statistics are derived comparing the profiling LiDAR with the DSM and DTM product, as well as LiDAR measurements at the cross-over points where LiDAR data was collected at different dates, see Table 3. The purple boxes indicate the location of the comparison profiles shown in Fig. 5 and Fig. 6.

Table 3. LiDAR cross-over points statistics. The repeat accuracy (RMSE) of the LiDAR measurements is below 40 cm. The absolute error budget is dominated by GPS/INS solution errors, as well as imprecision of the planimetric location due to roll and pitch errors in the order of half the spot size, leading to vertical error for points on slopes. The terrain slopes are computed using NED data. Coordinates are in Alaska Albers projection, Geoid09 orthometric height.

#	Date	X (m)	Y (m)	LiDAR (m)	Slope (deg)	Cross-over abs. Difference (m)
1	7/12/2010	209627.98	1542720.20	639.28	2.5	**0.04**
	7/30/2010	209628.00	1542720.20	639.24		
2	7/22/2010	219174.86	1275031.35	7.95	2.0	**0.10**
	7/12/2010	219174.86	1275031.36	7.85		
3	7/12/2010	302192.54	1347972.49	1694.77	22.3	**0.29**
	7/23/2010	302192.54	1347972.50	1694.48		
4	7/16/2010	131834.79	1446011.48	5210.37	15.8	**0.36**
	7/18/2010	131834.77	1446011.46	5210.01		
5	7/12/2010	318893.86	1509559.97	1170.00	14.3	**0.05**
	7/23/2010	318893.87	1509559.97	1170.05		
6	7/19/2010	402357.82	1291967.64	1440.95	4.7	**0.02**
	7/1/2210	402357.82	1291967.63	1440.97		
7	7/12/2010	181351.92	1539919.20	752.47	17.7	**1.02**
	7/30/2010	181351.92	1539919.21	751.45		
8	7/12/2010	279149.14	1549483.72	1413.77	10.1	**0.32**
	7/30/2010	279149.13	1549483.73	1414.09		
9	7/12/2010	338202.09	1339715.54	781.68	6.3	**0.30**
	7/19/2010	338202.09	1339715.53	781.38		
10	7/12/2010	317513.07	1336550.40	1331.63	19.9	**0.16**
	7/23/2010	317513.07	1336550.39	1331.79		
					Average (m)	**0.27**
					Stdev (m)	**0.29**
					RMSE (m)	**0.39**

Vertical Accuracy

The available 12,628,042 LiDAR points were sub-sampled by a factor 200 to reduce the amount of points and create a sampling density of approximately 5 m; the same as the DEM products. Secondly, LiDAR returns from water bodies were removed using the water mask created for this project as a deliverable, leaving a total of 48,433 LiDAR points. These points were used to validate the accuracy of the DSM and DTM product, without further culling, see Table 4 and Table 5.

The estimated overall RMSEz is 1.46 m for the DSM and 1.54 m for the DTM, respectively, derived using these 48433 LiDAR points at all slopes and terrain, without performing any further culling. Approximately 33% (16249 of 48433) of the points are located at terrain slopes greater than 10°. The RMSEz is well within product specification for the DTM, see Table 5, with RMSEz=1.11 m for slopes between 0° and 10°, and as good as RMSEz=3.44 m for terrain slopes of more than 30°, based on 2035 points.

As can be seen from Table 4 and Table 5, the average difference between the LiDAR points and DEM products is close to zero for the moderate terrain slopes, and increasing for larger terrain slopes, approximately 1m for the severe terrain slopes, the LiDAR elevation being higher. As part of the standard production process the data are slightly spatially filtered with a very small kernel to reduce noise, and we speculate that this could be the cause of this slight bias that increases with slope. Note that a number of these LiDAR points on the extreme flat terrain were used to generate the product, as well as for this validation. For product generation, LiDAR points are automatically selected that are believed to be in flat and open, bare-earth, areas (by thresholding on the terrain slope derived from the LiDAR and checking the three recorded LiDAR returns elevation and magnitude). Approximately 350 points that

fulfilled the thresholds were used to determine a single z-bump of the DEM product to best fit the average LiDAR elevation at these points. Also note that the LiDAR data were acquired at different times than the radar data to generate the DEM products, because the LiDAR is nadir looking, while the radar is side-looking.

Table 4. Vertical accuracy assessment of the DSM product for the Pilot Area based on LiDAR data (not culled).

Slope	0° – 10°	10° – 20°	20° – 30°	30°+	Overall
Number of Points	32184	10358	3856	2035	**48433**
Average (m)	-0.12	0.63	0.98	1.16	**0.18**
Standard Deviation (m)	1.10	1.55	1.71	3.04	**1.45**
Minimum difference (m)	-8.04	-17.90	-7.50	-52.88	**-52.88**
Maximum difference (m)	16.35	11.48	15.96	25.07	**25.07**
RMSE (m)	**1.13**	**1.64**	**1.97**	**3.25**	**1.46**

Table 5. Vertical accuracy assessment of the DTM product for the Pilot Area based on LiDAR data (not culled).

Slope	0° – 10°	10° – 20°	20° – 30°	30°+	Overall
Number of Points	32184	10358	3856	2035	**48433**
Average (m)	0.08	0.88	1.23	1.20	**0.40**
Standard Deviation (m)	1.11	1.55	1.79	3.12	**1.49**
Minimum difference (m)	-8.01	-17.13	-7.27	-52.60	**-52.60**
Maximum difference (m)	16.87	11.65	16.18	25.05	**25.05**
RMSE (m)	**1.11**	**1.78**	**2.17**	**3.44**	**1.54**
Product spec. RMSE (m)	**1.85**	**3.70**	**5.55**	**7.40**	

Horizontal Accuracy

The planimetric accuracy of the product is typically assessed using deployed corner reflectors that are surveyed within a few cm on the ground using GPS technology. These corner reflectors are then measured in the delivered products to be within a few meters from their surveyed locations, well within the deliverable product specification of RMSEr=8.03 m. In this paper, LiDAR profiles over mountain ridges are used to demonstrate the horizontally accuracy of the GeoSAR data. The horizontal pointing accuracy (RMSE) of the calibrated LiDAR is accurate to approximately half the spot size, approximately 1.5 m in along and across track direction. For example, for a 10° terrain slope, if the horizontal pointing error would be 1.5 m (i.e., an actual error in the estimated horizontal coordinates of the LiDAR point), then this would translates to a vertical error of $1.5 \times \tan(10°) = 0.26$ m, which in turn would contribute negatively to the vertical accuracy assessment, i.e., the IFSAR vertical accuracy is underestimated in sloped terrain if there are LiDAR pointing errors in the method used in this paper. However, it becomes clear from the analysis of the LiDAR cross-over points on sloped terrain that the vertical error due to horizontal uncertainties is quite small, see Table 3.

Fig. 5 and Fig. 6 show an East-West and a North-South profile comparison between the GeoSAR IFSAR DSM and LiDAR data over mountain peaks in steep terrain. The locations of these profiles are indicated in the overview Fig. 4 by the purple boxes. It can be concluded from these profiles that the location of GeoSAR IFSAR data is accurate in mountainous terrain and that the shape of the slopes is very well traced by the IFSAR data.

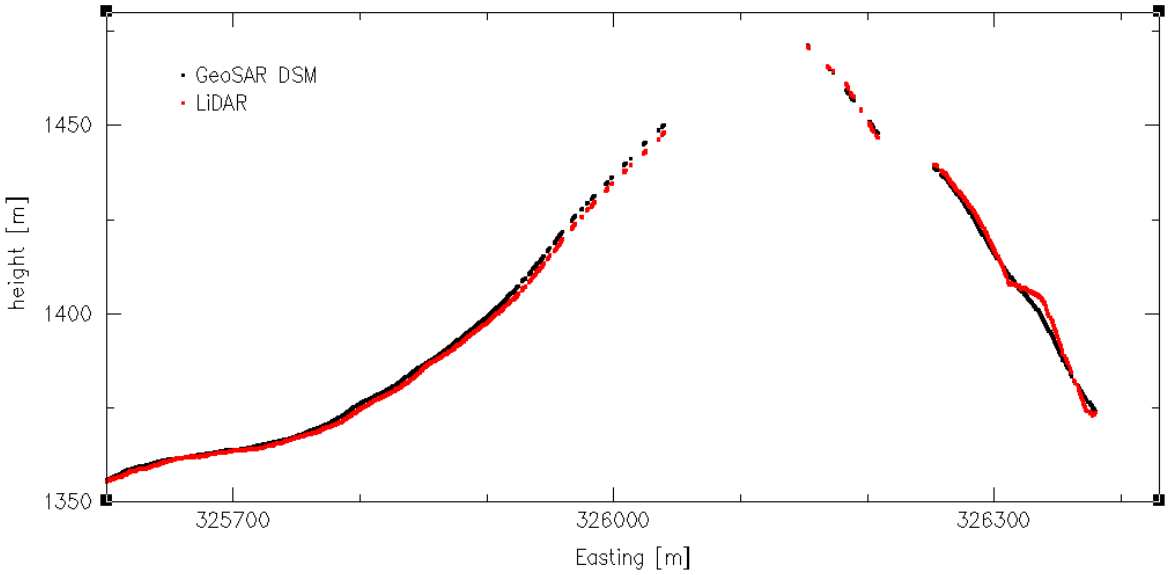

Figure 5. LiDAR profile for an East-West line over mountainous terrain with terrain slopes of ~10°–25°. The difference between the LiDAR and the DSM is approximately 1.5 m. It can be clearly seen that the DSM aligns well with the LiDAR profile data, and that mountain ridges are correctly located in the IFSAR data.

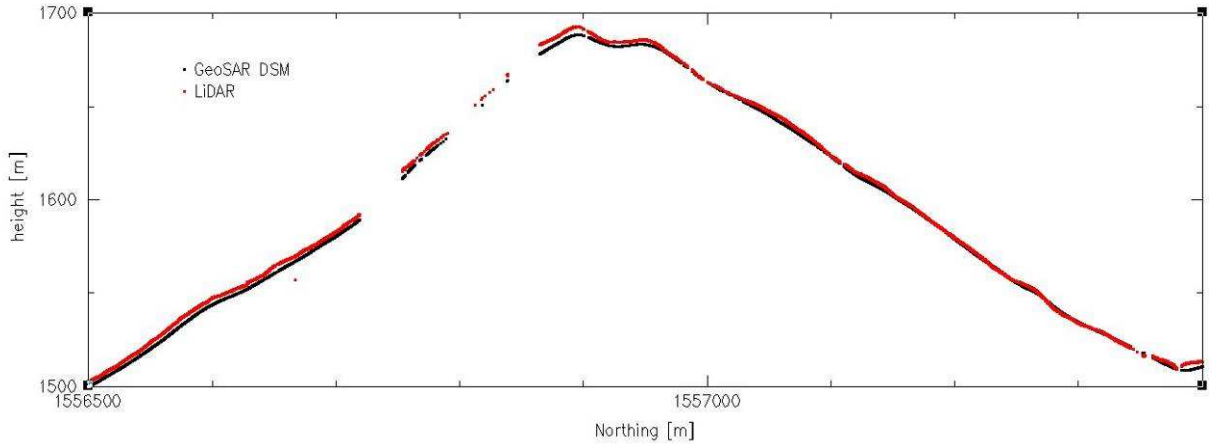

Figure 6. North-South LiDAR profile over mountainous terrain with terrain slopes of ~25°. The difference between the LiDAR and the DSM is ~2.5 m on the slope and ~3.5 m at the peak. It can be clearly seen that the DSM aligns well with the LiDAR profile data, and that mountain ridges are correctly located in the IFSAR data.

ACKNOWLEDGEMENTS

The authors acknowledge the many contributions made by the engineering, scientific and supporting staff of Fugro EarthData. In particular we would like to thank K. Cubbage for creating the ArcGIS figures and B. Beavers and B. Downey for performing the LiDAR analysis. Also acknowledged are Alaska Aerofuel and the many people at the University of Alaska, Fairbanks, for their hospitality during our data acquisition in summer of 2010, as well as to D. Maune and others at Dewberry for asking insightful questions, performing data analysis, and providing comments.

CONCLUSIONS

The processing of the Alaska Project Area 2010 acquired data is well underway and on track to deliver the products well within the accuracy specification. The described GeoSAR IFSAR advantages and suitability to the mixed terrain types and extreme topography are proved to be an efficient solution for accurate large area mapping. The overall RMSEz of the data over flat and rough terrain was estimated to be 1.46 m for the DSM and 1.54 m for the DTM, using 48,433 LiDAR ground control points, of which 33% are located on terrain slopes of more than 10°.

REFERENCES

EarthData. Results of LiDAR Validation Flight over Georgia and South Carolina. Internal Technical Report, Dec. 6, 2011.

Hoffman, G.R. Integration of a Profiling LiDAR with GeoSAR. In: *Proceedings of the ASPRS Annual Conference*, Reno, Nevada, USA, May 1-5, 2006.

Kampes, B.M. *Radar Interferometry: Persistent Scatterer Technique*. Volume 12 in the series on Remote Sensing and Digital Image Processing. Springer, Berlin, 2006.

Maune, D.F. Digital Elevation Model (DEM) Data for the Alaska Statewide Digital Mapping Initiative (SDMI), www.alaskamapped.org, listed under DEM Workshop Whitepaper, September 18, 2008.

Maune, D.F. Alaska Statewide Digital Mapping Initiative: Mapping Alaska for the First Time. In: *Proceedings of the ASPRS/ MAPPS 2009 Fall Conference*, San Antonia, Texas, USA, Nov. 16-19, 2009.

Maune, D.F. Alaska Statewide DEM Collection Overview. In: *Proceedings of the ASPRS 2010 Conference*, Milwaukee, Wisconsin, USA, May 1-5, 2010.

Meyer, F. B.M. Kampes, R. Bamler, J. Fischer. Methods for Atmospheric Correction in INSAR Data. In: *Proceedings of Fringe Conference*, Frascati, Italy, 2005.

Morgan, K., B.M. Kampes, M. Blaskovich, M. Sanford. *Fugro's GeoSAR IFSAR Mapping Technology for Snow and Ice Penetration*. Presentation at the 45th Annual Alaska Surveying and Mapping Conference, Anchorage, Alaska, USA, Feb. 21-25, 2011

Reis, J.J., M.L. Williams, S. Hensley, D. Woods. Updating GeoSAR for Full-Pol Interferometric Capability. In: *Record of the IEEE International Radar Conference*, Pasadena, California, USA, May 4-8, 2009.

Rosen, P.A., S. Hensley, I. R. Joughin, et al., "Synthetic aperture radar interferometry," *Proc. IEEE*, vol. 88, no. 3, pp. 333-382, 2000.

Williams, M.L., M. Silman, S. Saatchi, S. Hensley, M. Sanford, A. Yohannan, B. Kofman, J. Reis, B.M. Kampes. *Analysis of GeoSAR, Dual-Band, INSAR Data for Peruvian Forest.* In: *International Geoscience and Remote Sensing Symposium*. pp. 1398-1401, Honolulu, HI, USA, July 25-30, 2010.

Wheeler, A. K., S. Hensley. The GeoSAR Airborne Mapping System. pp. 831-835, In: *Record of the IEEE International Radar Conference*, 2000.